Air, Sea, and Land Interactions of the Continental U.S. Hydroclimate

VASUBANDHU MISRA* AND P. A. DIRMEYER

Center for Ocean–Land–Atmosphere Studies, Calverton, Maryland

(Manuscript received 18 December 2007, in final form 8 July 2008)

ABSTRACT

Multidecadal simulations over the continental United States by an atmospheric general circulation model coupled to an ocean general circulation model is compared with that forced by observed sea surface temperature (SST). The differences in the mean and the variability of precipitation are found to be larger in the boreal summer than in the winter. This is because the mean SST differences in the two simulations are qualitatively comparable between the two seasons. The analysis shows that, in the boreal summer season, differences in moisture flux convergence resulting from changes in the circulation between the two simulations initiate and sustain changes in precipitation between them. This difference in precipitation is, however, further augmented by the contributions from land surface evaporation, resulting in larger differences of precipitation between the two simulations. However, in the boreal winter season, despite differences in the moisture flux convergence between the two model integrations, the precipitation differences over the continental United States are insignificant. It is also shown that land–atmosphere feedback is comparatively much weaker in the boreal winter season.

1. Introduction

The use of coupled land–ocean–atmosphere models is growing in the community as a tool for both climate research (e.g., Meehl et al. 2007 and references therein) and prediction (Saha et al. 2006). With increasing and improving computing resources, it is now possible to run these coupled models with relative ease.

Traditionally, most land–atmosphere interaction studies have been conducted either with offline land models (e.g., Berg et al. 2003; Dirmeyer et al. 2006; Trenberth et al. 2007) or a land model coupled to an atmospheric general circulation model (AGCM; Shukla and Mintz 1982; Xue et al. 1991; Koster et al. 2004; Dirmeyer 2005). These studies have been extremely helpful in realizing the importance of land–atmosphere interactions on climate predictability and variability. However, it is also being realized that, in a coupled system of interacting oceans, land, and atmosphere, the remote influences of, for instance, land use land cover change (Voldoire and Royer 2005), or the remote effect of stratus clouds over the eastern oceans (Misra and Marx 2007) are diagnosed differently from when component models are forced with observed variations at their boundaries. Furthermore, forced systems are artificial. These reduced component systems were appropriate at the time of their introduction when computing resources were a serious limiting factor. Such model configurations cannot exhibit the full range of possible feedbacks between components of the climate system.

Whereas studies of ocean–atmosphere interactions have focused on the tropics, a favorite region of study for land–atmosphere interactions is over the U.S. Great Plains. The Great Plains was found to be one of the ‘‘hot spots’’ for relatively high land–atmosphere coupling strength in several AGCMs (Koster et al. 2006). Other regions that showed similar strong coupling strengths in that study were the Sahel in West Africa and the Asian monsoon regions. Guo et al. (2006), in examining the land–atmosphere coupling strengths in several AGCMs, found that these ‘‘hot spots’’ occur in the transition zones between dry and wet areas. These transition zones were identified as unique regions in the globe where the surface evaporation variations are relatively high. They

* Current affiliation: Department of Meteorology, The Florida State University, Tallahassee, Florida.

Corresponding author address: Vasubandhu Misra, Department of Meteorology, The Florida State University, 404 Love Building, Tallahassee, FL 32306.
E-mail: vmisra@fsu.edu

DOI: 10.1175/2008JHM1003.1

were strongly correlated to soil moisture that results in land states having strong influence on precipitation.

The U.S. Great Plains has received considerable attention in observational as well as modeling studies (e.g., Trenberth and Guillemot 1996; Higgins et al. 1999; Nigam et al. 1999; Dominguez and Kumar 2005; Ruiz-Barradas and Nigam 2006). In a recent model analysis of the warm season rainfall variability over the U.S. Great Plains, Ruiz-Barradas and Nigam (2005) showed that rainfall variability and its amplitude are poorly represented in both the atmospheric reanalysis products and forced AGCM simulations. An important finding was that the models were poorly representing the interaction pathways of water sources over the U.S. Great Plains, with surface evaporation being clearly overestimated (Ruiz-Barradas and Nigam 2005, 2006).

In this paper, we compare the results of two identical AGCM simulations over the contiguous United States, with one AGCM forced with observed SST and the other coupled to an ocean general circulation model (OGCM). The objectives of this study are twofold: 1) to find if there is any influence on air–sea coupling over the continental United States and 2) to understand the differences (if any) between the two model runs.

In the following section, a brief description of the model is provided. This is followed by an explanation of the conducted experiments in section 3. The results are presented in section 4, followed by concluding remarks in section 5.

2. Model description

The Center for Ocean–Land–Atmosphere Studies' (COLA) coupled climate model (Misra et al. 2007; Misra 2007; Misra and Marx 2007) is used in this study. It consists of AGCM version 3.2 at a spectral resolution of T62 with 28 sigma levels, identical to the National Centers for Environmental Prediction–National Center for Atmospheric Research's (NCEP–NCAR's) reanalysis model (NCEPR; Kalnay et al. 1996). The dynamical core follows from the Eulerian core of the community climate model version 3 (Kiehl et al. 1998), wherein the dependent variables are spectrally treated except for moisture, which is advected by semi-Lagrangian scheme. The relaxed Arakawa–Schubert scheme (Moorthi and Suarez 1992; Bacmeister et al. 2000) is used for deep convective parameterization. The longwave and shortwave radiation schemes are identical to those in the community climate system model version 3.0 (Collins et al. 2006). The clouds are diagnosed following Slingo (1987). The cloud optical properties follow from Kiehl et al. (1998). The planetary boundary layer is a nonlocal scheme (Hong and Pan 1996), and the shallow convection uses the formulation in Tiedtke (1984). The land surface scheme uses the Simplified Simple Biosphere scheme (SSiB; Xue et al. 1991, 1996; Dirmeyer and Zeng 1999).

The COLA AGCM is coupled to the modular ocean model version 3.0 (MOM3; Pacanowski and Griffies 1998), which covers the global oceans between 74°S and 65°N with realistic bottom topography. However, ocean depths less than 100 m are set to 100 m, and the maximum depth is set to 6000 m. The artificial high-latitude meridional boundaries are impermeable and insulating. It has a uniform zonal resolution of 1.5°, while the meridional resolution is 0.5° between 10°S and 10°N, gradually increasing to 1.5° at 30°N and 30°S and fixed at 1.5° in the extratropics. The vertical mixing is the nonlocal K-profile parameterization of Large et al. (1994). The momentum mixing is the space–time dependent scheme of Smagorinsky (1963), and tracer mixing follows Redi's (1982) and Gent and McWilliams's (1990) quasi-adiabatic stirring.

3. Design of experiments

The coupled model results presented here are from the last 42 yr of a 100-yr integration that was restarted from a previous coupled model integration (Misra and Marx 2007). The coupled mean state of the model is, therefore, well spun-up. This experiment is hereafter referred to as COUPLED.

Similarly, the AGCM identical to that used in the COUPLED experiment is integrated for 100 yr from 1901 to 2000, with observed SST from optimally interpolated version 2 (OI2) from Reynolds et al. (2002). The atmospheric and land initial conditions are realized from a previous restart file of the AGCM, which is redated to 0000 UTC 1 January 1901. The results are analyzed from the last 42 yr of this integration. This experiment is hereafter called UNCOUPLED.

In addition to comparing the two model simulations during the boreal summer season of June–August (JJA), we will also be contrasting it with the boreal winter season of December–February (DJF). The motivation for the analysis of the comparison in the two seasons is to illustrate the role of the land surface state in augmenting the divergence of the solutions between the two models. In the JJA season, the land surface over the continental United States is warmer and hydrologically more active (with surface evaporation closely associated with soil moisture and precipitation). In contrast, in the DJF season, the land surface is relatively cold (nearly at or below freezing temperatures over the U.S. Great Plains), and the evaporation is relatively decoupled from both precipitation and soil moisture variations. Furthermore, in the DJF season, the precipitation is more of a large-scale nature (arising from grid-scale saturation) than from being convective, as observed in the boreal summer season.

4. Results

We will be validating the model simulations with the most recent version of the Global Offline Land Surface Dataset (GOLD; Dirmeyer and Tan 2001), which is available at the same T62 resolution of our GCM simulations. Another attractive aspect of this validation dataset is that the same version of the SSiB land surface scheme that is used in the COUPLED and UNCOUPLED model integrations is also used to generate GOLD. This dataset is available from 1960 to 2002. The model validation is conducted for the 42 yr that overlap with GOLD. GOLD uses hybrid sets of meteorological forcing data that have been produced by combining the 40-yr European Centre for Medium-Range Weather Forecasts Re-Analyses (ERA-40) with the Global Precipitation Climatology Centre's (GPCC; Rudolf et al. 1994) monthly precipitation estimates. For the sake of consistency, we have used this GOLD precipitation dataset in our verification throughout this study. However, the results are nearly the same when we use the daily gridded precipitation analysis of Higgins et al. (2004). The data used in this study including the observations (GOLD) have been linearly detrended for the period of verification prior to any analysis. However, this procedure had no impact on the results.

a. Precipitation and SST climatology

In Figs. 1a,b, we show the climatological precipitation over land for the DJF and JJA seasons from GOLD (GPCC observations), respectively. The climatological precipitation errors of the COUPLED and UNCOUPLED runs are comparable in the DJF season (Figs. 1c,e,g). In the summer season (Figs. 1d,f), the errors are relatively larger than in the winter in both of the simulations. Furthermore, the COUPLED model shows some significant improvements in the JJA season over the Midwest region relative to the UNCOUPLED run (Fig. 1h). However, in the northeastern United States, the UNCOUPLED integration shows some marginal improvement over the COUPLED simulation.

In Figs. 2a,b, the climatological differences of SST between the COUPLED and the UNCOUPLED simulations for the two seasons are shown. These differences can also be called climatological seasonal errors of SST in the COUPLED simulation, as observed SST is used in the UNCOUPLED run. In Fig. 2, the SST errors, especially in the North American coastal regions, are comparable between the two seasons. Even the SST errors in the remote areas of the tropical Pacific, Indian, and Atlantic Oceans are qualitatively similar between the two seasons. Yet the differences in precipitation between COUPLED and UNCOUPLED simulations, as seen in Figs. 1g,h, are quite different in DJF and JJA seasons, respectively. Obviously, the influence of the quantitative differences in the SST errors of the remote ocean basins cannot be discounted. For example, the cold equatorial Pacific bias is more severe in the winter (Fig. 2a) than in the summer (Fig. 2b). Likewise, the warm bias in the southeastern Pacific and Atlantic Oceans is more severe in the summer than in the winter. It is, however, reasonable to query if the land surface processes are contributing to these summertime precipitation differences between the model simulations over the United States, given that the SST differences are somewhat comparable. A major difference between the two seasons is that both of the simulations have produced winter precipitation over the United States from large-scale processes rather than convective precipitation (Figs. 3a,c). In the summer season, the source of precipitation over the United States is nearly split in half between convective and nonconvective rainfall in both model simulations (Figs. 3b,d). Another important difference between the two seasons is the large difference in absolute humidity because of the nonlinear dependence of the saturation humidity on temperature. The warmer temperatures in the JJA season have higher water vapor content than in the DJF season. This feature explains in large part the large divergence of the precipitation between the simulations in the JJA season in Figs. 1h, and 3b,d relative to the DJF season (Figs. 1g and 3a,c). Another point to consider is that the COUPLED model does not include variations in the greenhouse gases, solar variability, volcanoes, and aerosols. The observed SST in the UNCOUPLED simulation has presumably all of these effects included. However, our analysis with the UNCOUPLED simulation using the output of the first half of the twentieth-century integration showed insignificant seasonal mean precipitation differences with the latter half of the twentieth-century integration, after the trend was removed.

The standard deviation of the seasonal mean precipitation for the two seasons from GOLD is shown in Figs. 4a,b. The corresponding differences in the standard deviation of the simulations from GOLD are shown in Figs. 4c–f. The differences are smaller in the winter compared to the summer in both of the simulations. This is also apparent when comparing Figs. 4g,h. However, the COUPLED simulation produces significantly more interannual variation than the UNCOUPLED

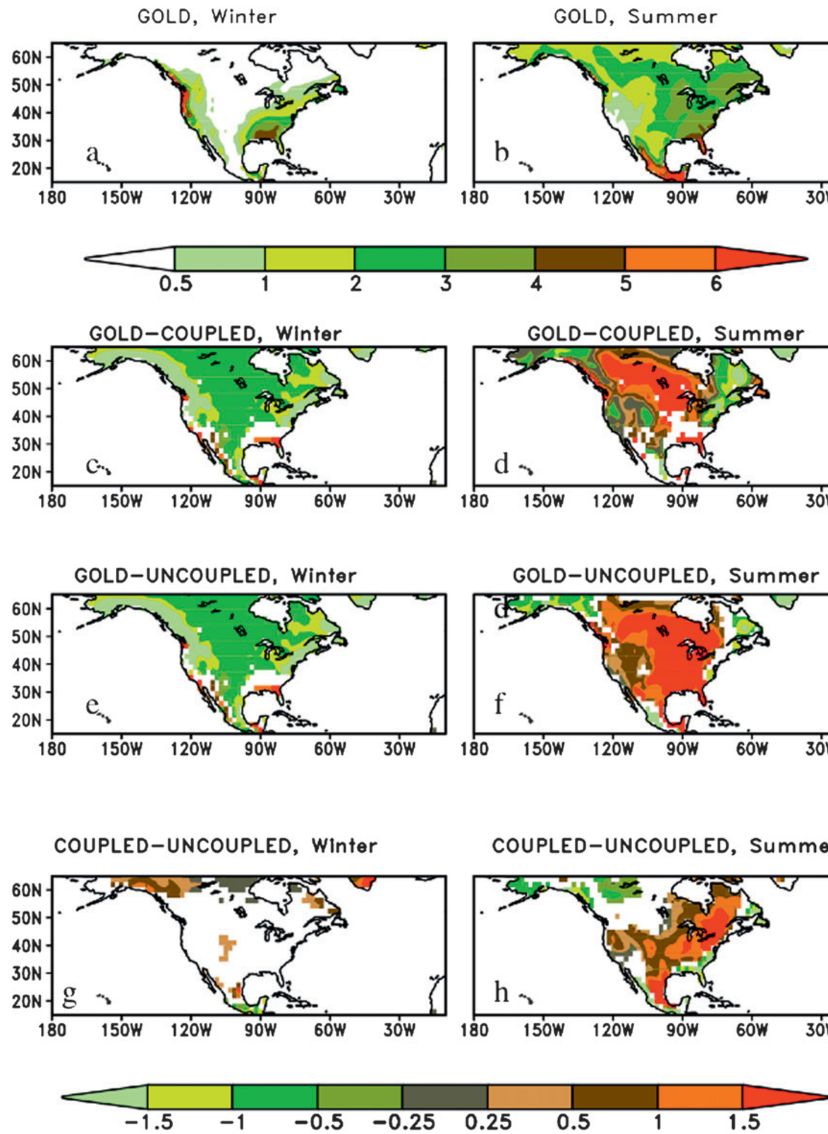

FIG. 1. Climatological (a) DJF and (b) JJA precipitation (mm day^{-1}) from GOLD. Climatological precipitation differences between GOLD and COUPLED for (c) DJF and (d) JJA. (e),(f) Same as (c),(d) but for GOLD and UNCOUPLED. (g),(h) Same as (e),(f) but for COUPLED and UNCOUPLED simulations. Only significant values at 90% confidence interval according to the *t* test are shaded in (c)–(h).

simulation in the central United States, albeit less than that in the GOLD analysis.

b. Surface evaporation

The surface evaporation rates in the winter and summer from GOLD are shown in Figs. 5a,b, respectively. The corresponding climatological errors in the COUPLED and UNCOUPLED runs are shown in Figs. 5c–f. Except over Central America and the southwestern United States, the climatological errors in surface evaporation are relatively larger in the summer (Fig. 5h) than in the winter (Fig. 5g) in both model runs. Like precipitation, the surface evaporation is underestimated in the central and eastern United States in both simulations. The COUPLED simulation exhibits larger surface evaporation over most parts of the United States in the summer than the UNCOUPLED simulation, bringing the former closer to the GOLD analysis. However, in the southeastern United States, the UNCOUPLED simulation is slightly better than the COUPLED simulation.

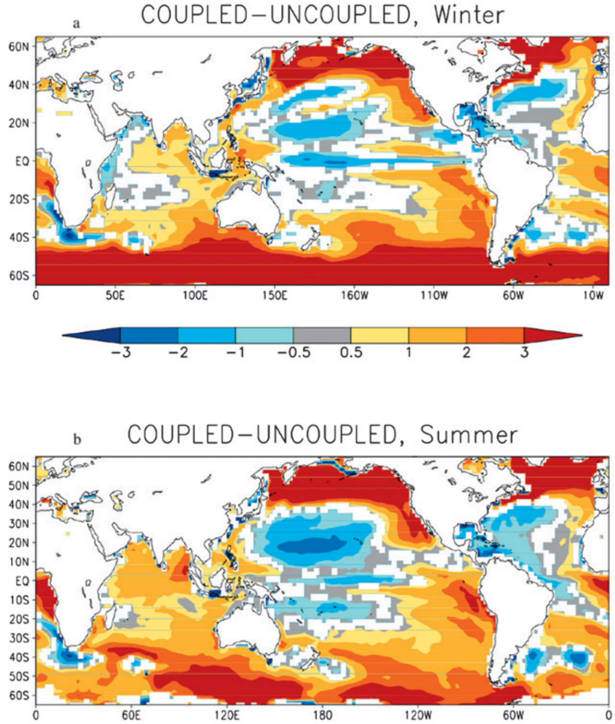

FIG. 2. Climatological differences of SST (°C) between COUPLED and UNCOUPLED simulations in (a) DJF and (b) JJA. The UNCOUPLED SST is from Reynolds et al. (2002). Only significant values at 90% confidence interval according to *t* test are shaded.

c. *Moisture flux convergence*

The climatological seasonal mean moisture flux convergence from GOLD for the DJF and the JJA seasons are shown in Figs. 6a,b, respectively. As noticed earlier with precipitation and evaporation, the errors of the moisture flux convergence in both simulations are comparable in the winter (Figs. 6c,e,g) and relatively smaller than that in the summer (Figs. 6d,f,h). In the JJA season, the UNCOUPLED run exhibits moisture flux divergence over parts of the midwestern United States contrary to either the GOLD analysis or the COUPLED simulation. However, the moisture flux divergence over parts of Indiana, Ohio, and Illinois in GOLD are poorly (well) replicated in the COUPLED (UNCOUPLED) simulation. Quantitatively, the COUPLED simulation exhibits comparable moisture flux convergence as GOLD, with ratios close to 1 in parts of the southwestern and midwestern United States in the summer season.

d. *Surface temperature*

The climatological winter and summer surface temperatures from GOLD are shown in Figs. 7a,b respectively. The temperatures over Mexico, and the southwestern, and the southeastern United States are colder in the COUPLED simulation relative to GOLD (Fig. 7c). Furthermore, surface temperatures north of the freezing line in the COUPLED run (Fig. 7c) are slightly warmer than GOLD (Fig. 7a) and the UNCOUPLED run (Figs. 7e,g), which is probably related to the higher extratropical SSTs in the COUPLED run (Fig. 2a). In the summer, the surface temperatures are generally warmer over the continental United States in the COUPLED simulation (Fig. 7d) compared to GOLD (Fig. 7b). The UNCOUPLED simulation in Figs. 7f,h exacerbates the errors of the corresponding COUPLED integration further with the exception over the Canadian Shield and parts of northwestern United States during summer.

e. *General circulation*

As a result of the air–sea coupling, there is a strong influence on the general circulation of the COUPLED simulation, which also contributes significantly to the differences from the UNCOUPLED integration. These mean circulation patterns serve as atmospheric bridges for remote surface boundary forcing (Nigam 2003). Furthermore, the differences in these upper-level planetary scale divergence patterns will have strong implications on the low-level convergence to maintain mass balance, which in turn will have strong implications on the differences in local moisture flux convergence and hydrological cycle.

In Fig. 8, we show the climatological 200-hPa velocity potential with the divergent wind vectors from the NCEP reanalysis, and the COUPLED and UNCOUPLED integrations for both seasons. In the boreal winter, the upper-level convergence over the tropical Atlantic and the Caribbean Sea in the COUPLED simulation (Fig. 8c) has a closer resemblance to the NCEP reanalysis (Fig. 8a) than the UNCOUPLED integration (Fig. 8e). However, over the tropical Indian Ocean, the COUPLED model tends to convect excessively, leading to an in situ bias of excessive upper-level divergence. In the boreal summer season, the upper-level convergence in the southern Atlantic and eastern Pacific Oceans is generally weaker in both model simulations compared to the NCEP reanalysis. But the excessive upper-level divergence over the North American monsoon region in the UNCOUPLED integration is somewhat ameliorated in the COUPLED run. Furthermore, the upper-level divergence in the Asian monsoon region is weaker in the UNCOUPLED simulation relative to either the COUPLED run or the NCEP reanalysis.

In Fig. 9, we show the regression of the global streamfunction at 850 hPa on the normalized (by its

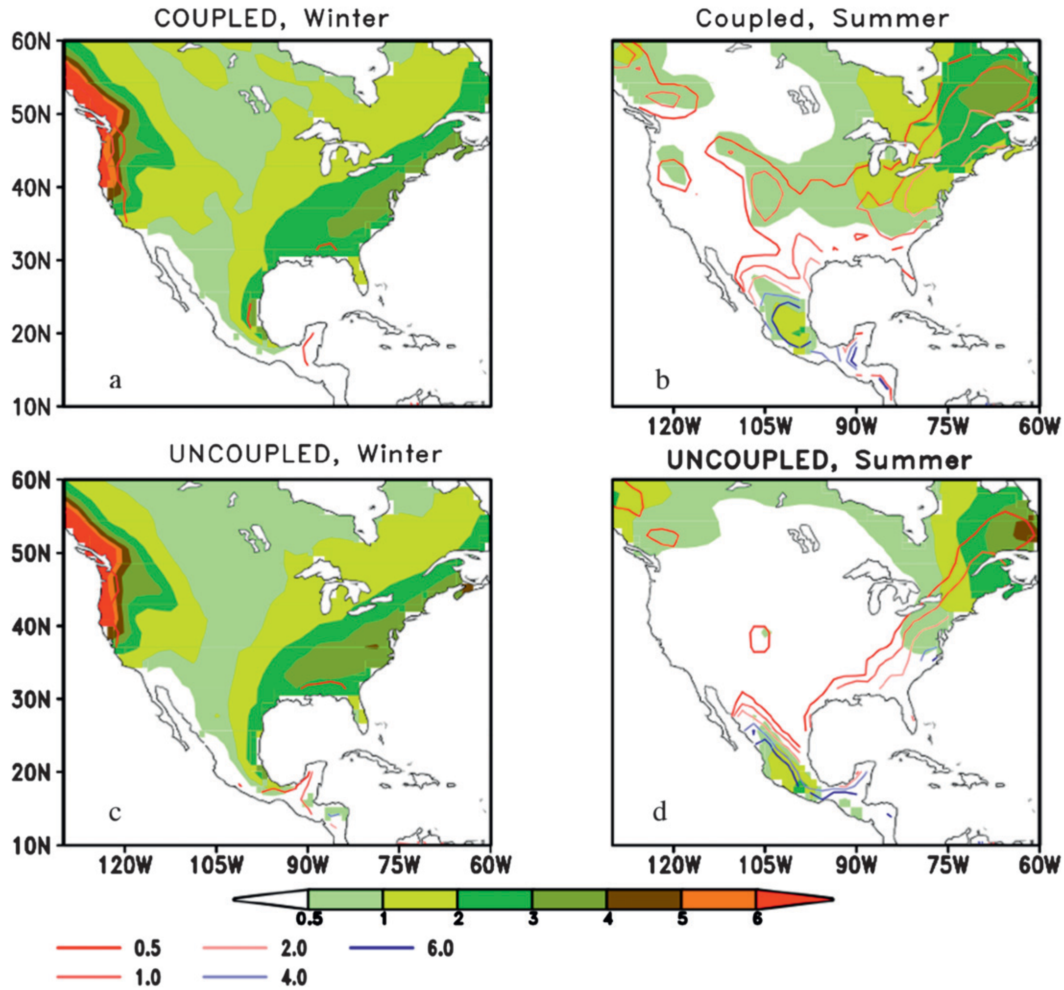

FIG. 3. Climatological large-scale (shaded) and convective (contoured) precipitation (mm day^{-1}) for (a),(c) DJF and (b),(d) JJA. The color of the contour intervals of convective precipitation is indicated in the legend.

corresponding standard deviation) Niño-3 SST index (5°N–5°S, 150°–90°W) for both seasons. In the boreal winter, the coupled run simulates the storm track variability in both hemispheres associated with the Niño-3 SST variability reasonably well compared with the NCEP reanalysis. In contrast, the corresponding variability of the streamfunction in the UNCOUPLED run is worse. The storm track variability in both hemispheres is relatively very weak in the UNCOUPLED integration. In the boreal summer season, the COUPLED run shows a deteriorated variability compared to the corresponding NCEP reanalysis. But the UNCOUPLED integration in the boreal summer season shows the low-level streamfunction anomalies over the northeastern Pacific and continental United States that is contrary (in the sign of the anomalies) to the NCEP reanalysis. These results are consistent with Misra (2008). It was shown there that air–sea coupling enhanced the variance in the COUPLED model relative to the UNCOUPLED model.

f. Land feedback

Thus far, we have shown that there are larger differences in the continental U.S. hydroclimate between the COUPLED and UNCOUPLED simulations in the summer season compared to the winter season. We contend that these differences between the model simulations in the summer season are augmented further by the land surface evaporation feedback on precipitation.

Koster et al. (2003) have succinctly split the land–atmosphere feedback into three parts: 1) wetting of soil by precipitation; 2) enhancement of evaporation by the wet soil; and 3) enhancement of precipitation by evaporation. The first part is obvious. The second part is supported in Fig. 10, which shows the contemporaneous correlations of precipitation with surface temperature.

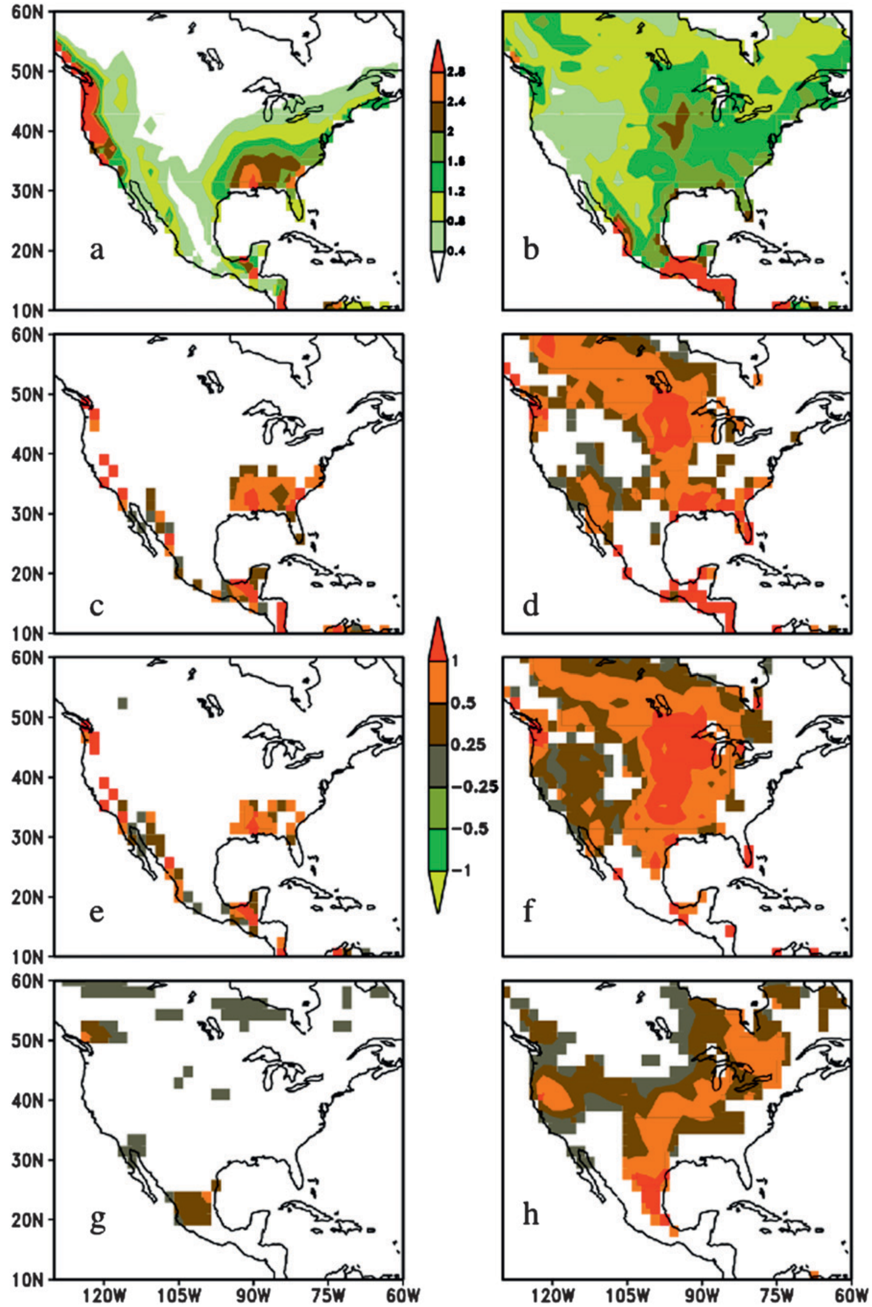

FIG. 4. Standard deviation of seasonal mean precipitation (mm day^{-1}) from GOLD for (a) DJF and (b) JJA. The difference in the seasonal mean standard deviation of precipitation between GOLD and COUPLED for (c) DJF and (d) JJA. (e),(f) Same as (c),(d) but for GOLD and UNCOUPLED. (g),(h) Same as (c),(d) but for COUPLED and UNCOUPLED. Only significant values at 90% confidence interval according to the *F* test are shown in (c)–(h).

In the boreal winter, these correlations are either insignificant or positive, suggesting that surface evaporation is not contributing to the precipitation which otherwise would lead to negative correlations, as seen in the boreal summer season (Figs. 10b,d,f). Here, the negative correlations induced by high precipitation suggests concomitant increased evaporation at the expense of sensible heat flux, which in turn induces cooler near-surface air temperatures (Huang and Van den Dool 1993).

The third part of the land–atmosphere feedback is more contentious (Koster et al. 2003). This is partly

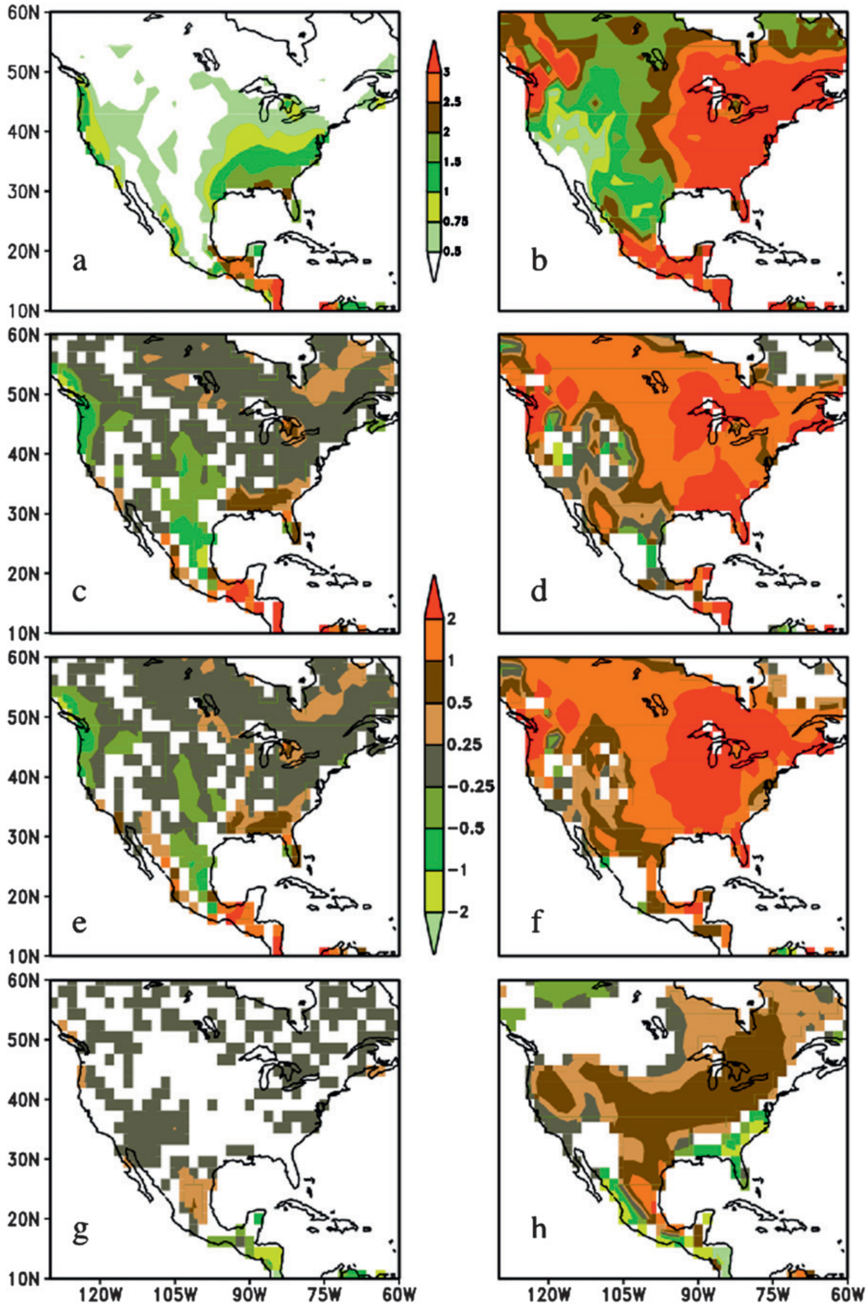

FIG. 5. Same as Fig. 1 but for surface evaporation.

because observations are limited. Furthermore, it is extremely difficult to extricate the causality between two variables that mutually influence each other. A common approach in the past has been to compare two AGCM simulations, one in which the land feedback to atmosphere is artificially shut off (Koster et al. 2003; Dirmeyer 2005). There are a number of caveats to this approach, including the lack of consideration of the influence of remote forcing and change in the general circulation (or the mean climate) of the "no land feedback" sensitivity run. Furthermore, in a coupled ocean–land–atmosphere framework, the plausibility of SSTs changing as a result of "no land feedback" can defeat the purpose of isolating the land feedback contribution to climate anomalies. In this study, we shall, therefore, resort to diagnostics that will serve to support at least qualitatively the idea of land–atmosphere feedback on the continental scale as an important contributor to the divergence of the

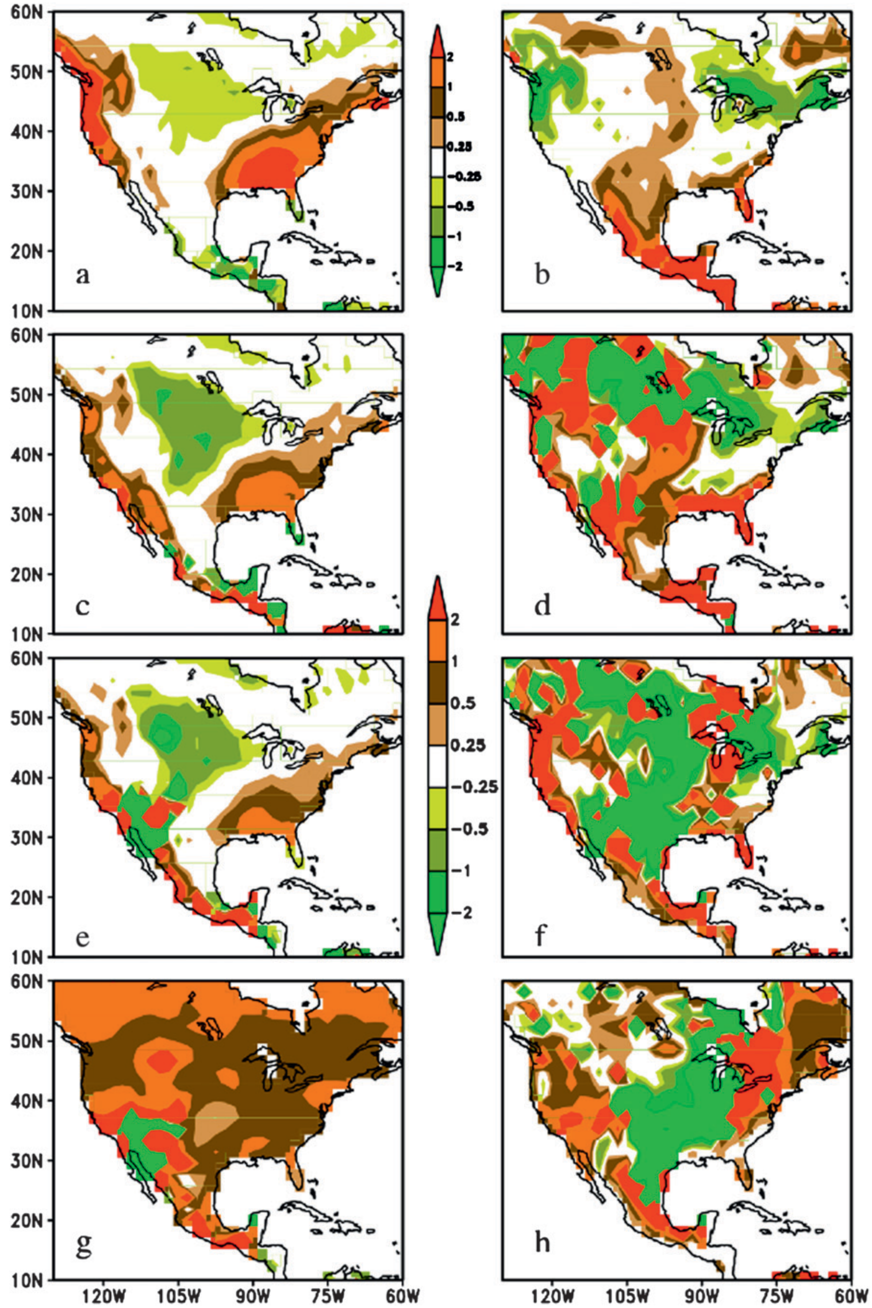

FIG. 6. Climatological moisture flux convergence (mm day^{-1}) in GOLD for (a) DJF and (b) JJA. The ratio of the climatological moisture flux convergence from the GOLD over COUPLED simulation (GOLD/COUPLED) in (c) DJF and (d) JJA. (e),(f) Same as (c),(d) but for GOLD/UNCOUPLED simulation. (g),(h) Same as (e),(f) but for COUPLED/UNCOUPLED.

solutions between the COUPLED and UNCOUPLED simulations.

In Fig. 11, we show the contemporaneous correlation of surface evaporation with precipitation for both seasons. In the GOLD analysis and in the COUPLED simulation, large parts of the midwestern United States have insignificant correlations during winter (Figs. 11a,c), which change to significantly larger positive correlations during summer (Figs. 11b,d). High correlation is a mark of aridity. The lack of adequate precipitation over land in the model puts more of the continent in the arid regime than is observed.

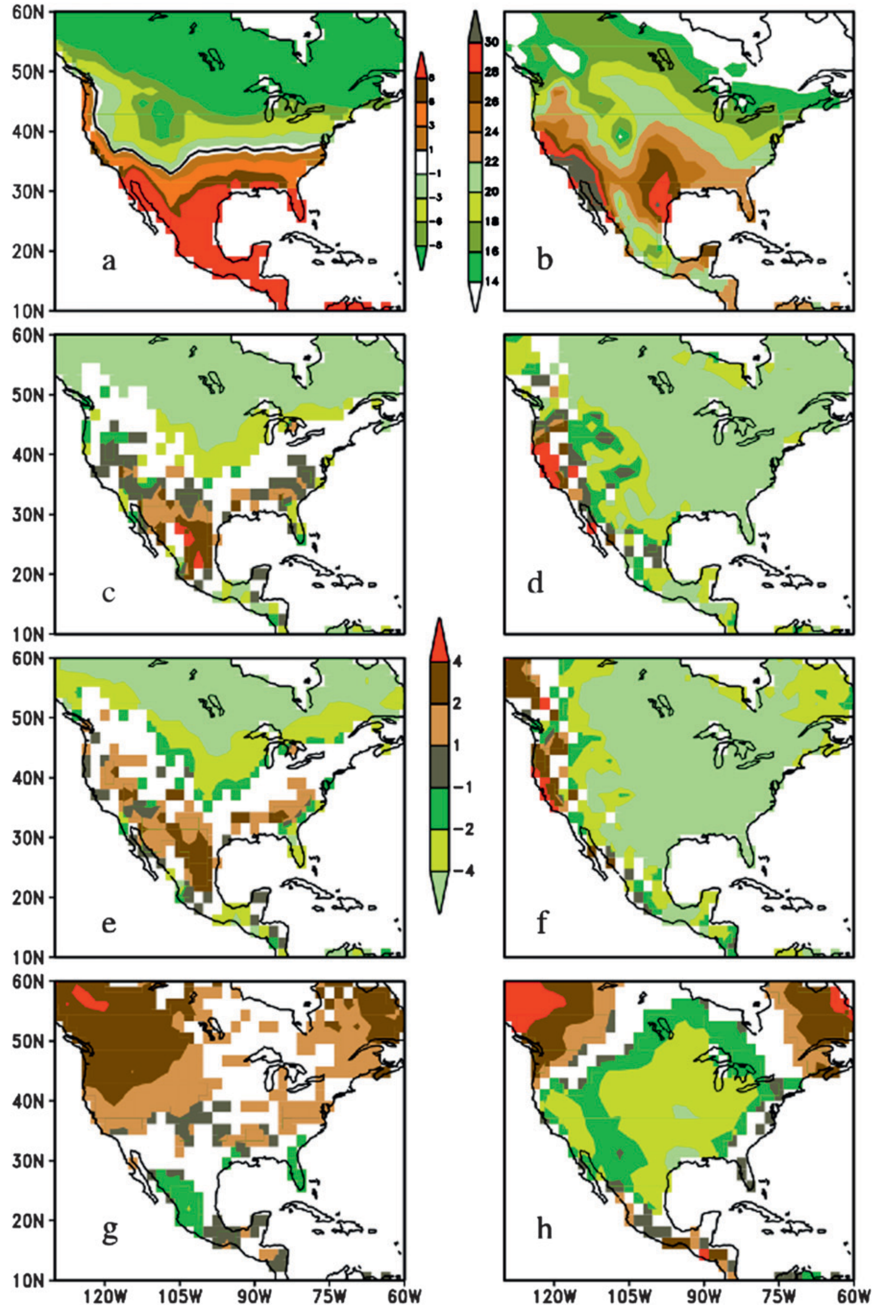

FIG. 7. Same as Fig. 1 but for surface temperature (°C). The freezing line is shown as a thick black line in (a).

These patterns of correlations are replicated when surface evaporation is correlated with root zone soil wetness (not shown). This may be interpreted following Guo et al. (2006), suggesting that in the model during the boreal winter, over most parts of United States, evaporation is energy limited, while in the boreal summer season evaporation is moisture limited. This happens largely because a larger fraction of the precipitation over the U.S. Great Plains during JJA is convective (Fig. 3), which is conceived to be the coupling agent between the land surface fluxes and precipitation (Guo et al. 2006). This is further corroborated in Fig. 12, which shows the contemporaneous correlations of downwelling shortwave flux at the surface with evaporation. In the boreal winter season in the COUPLED model (Fig. 12c), it is seen that the surface evaporation

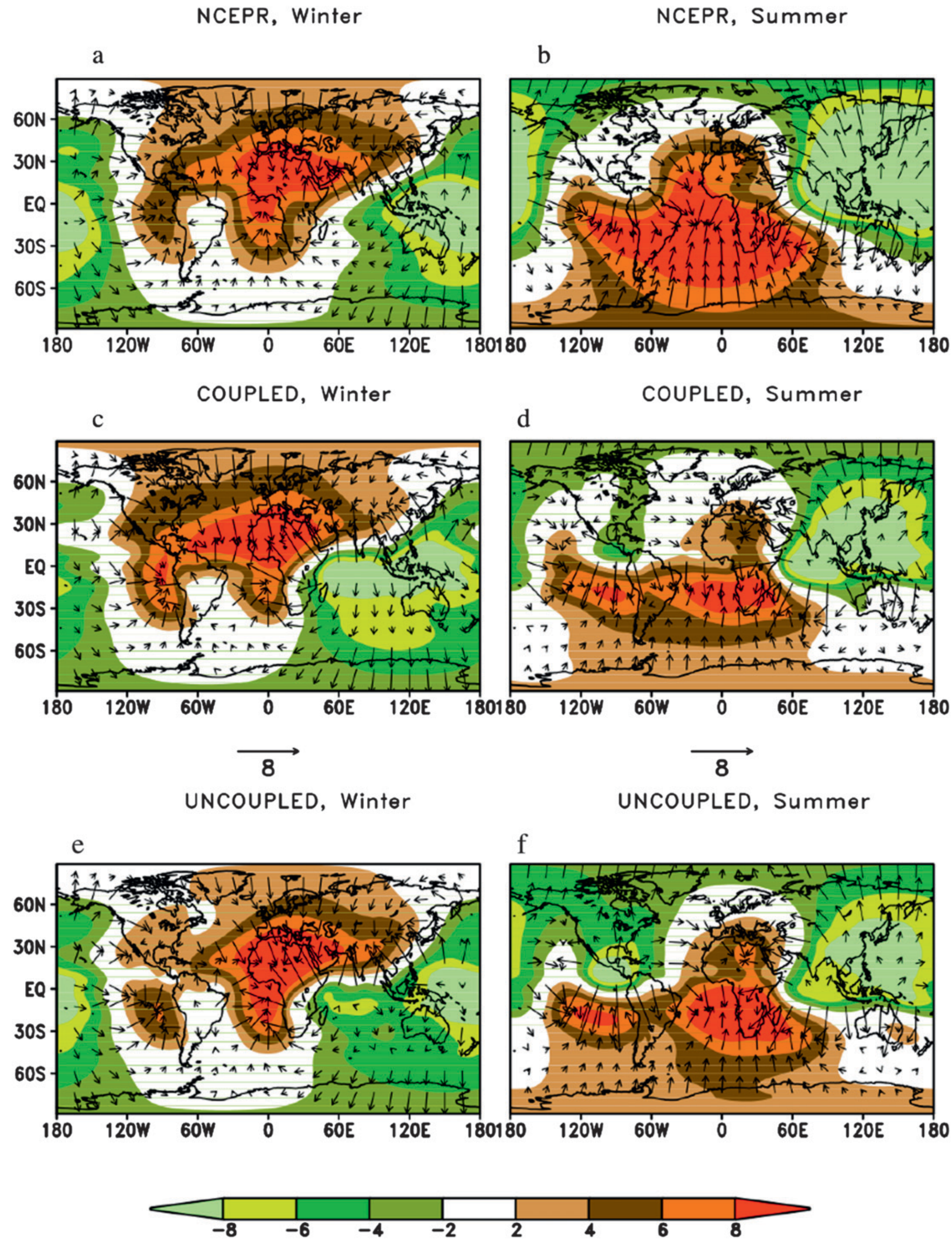

FIG. 8. Climatological velocity potential (1.0×10^{-6} m^2 s^{-1}) and divergent winds (m s^{-1}) at 200 hPa from (a),(b) NCEPR (Kalnay et al. 1996), and (c),(d) COUPLED and (e),(f) UNCOUPLED simulations in DJF and JJA, respectively.

increases (decreases) with increase (decrease) in the downwelling shortwave flux over most parts of United States, suggesting that evaporation is energy limited. This relationship flips into an inverse relation in the boreal summer season (Fig. 12d) when evaporation is moisture limited. However, the COUPLED model bias is clearly noticeable in comparison to the corresponding GOLD analysis (Figs. 12a,b). The UNCOUPLED model also exhibits similar change in sign in the correlations between the seasons (Figs. 12e,f). However, the

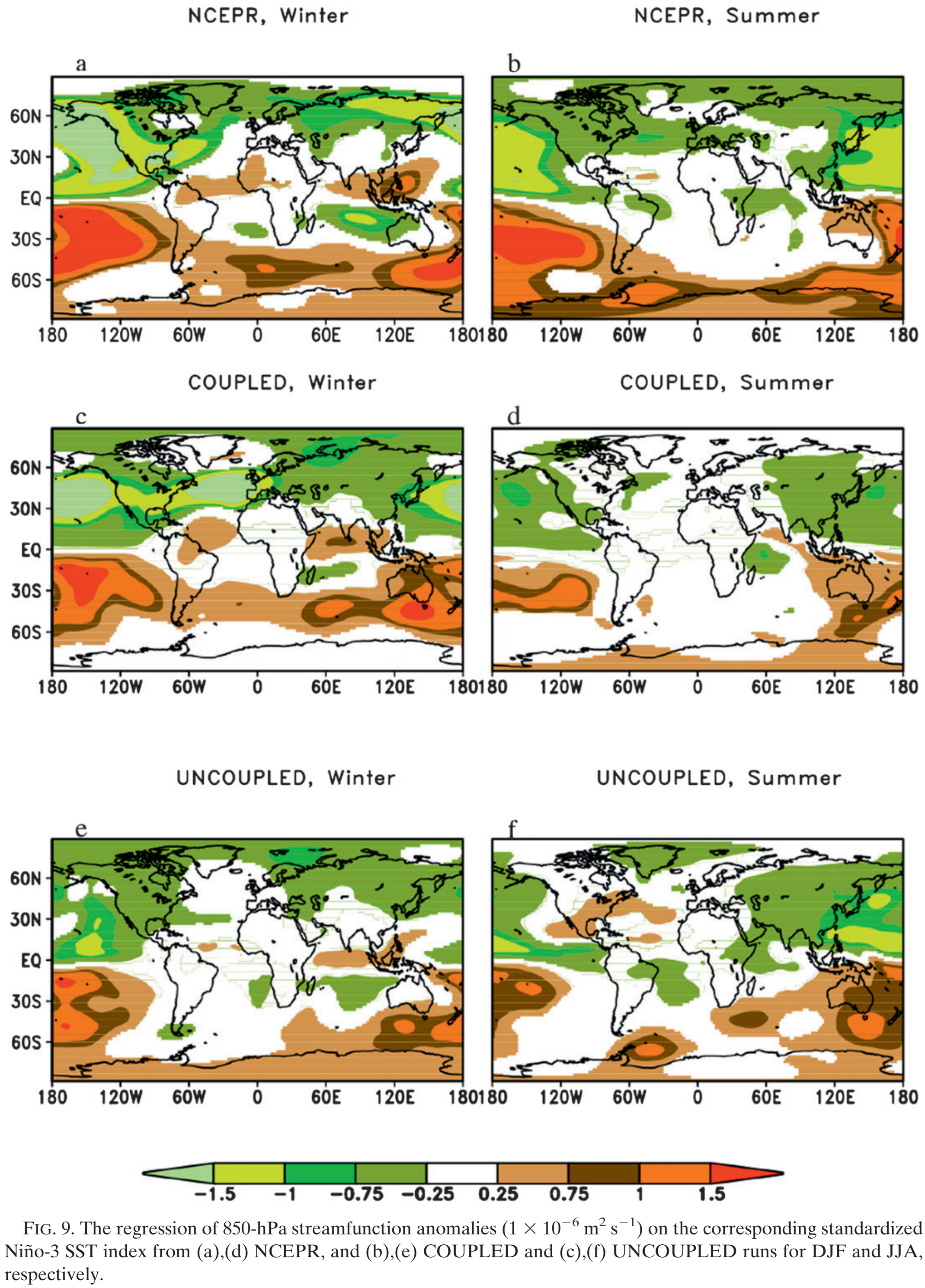

FIG. 9. The regression of 850-hPa streamfunction anomalies (1×10^{-6} m^2 s^{-1}) on the corresponding standardized Niño-3 SST index from (a),(d) NCEPR, and (b),(e) COUPLED and (c),(f) UNCOUPLED runs for DJF and JJA, respectively.

correlations are relatively weak compared to the COUPLED model. In other words, during JJA, the land surface evaporation in both models further accelerate the hydrological cycle over most parts of the United States relative to DJF. It may be noted that in Figs. 10–12, the correlations are qualitatively similar in both models, suggesting that land–atmosphere interaction physics is robust.

To address this issue of the role of the land–atmosphere feedback further, we have plotted in Fig. 13, akin to

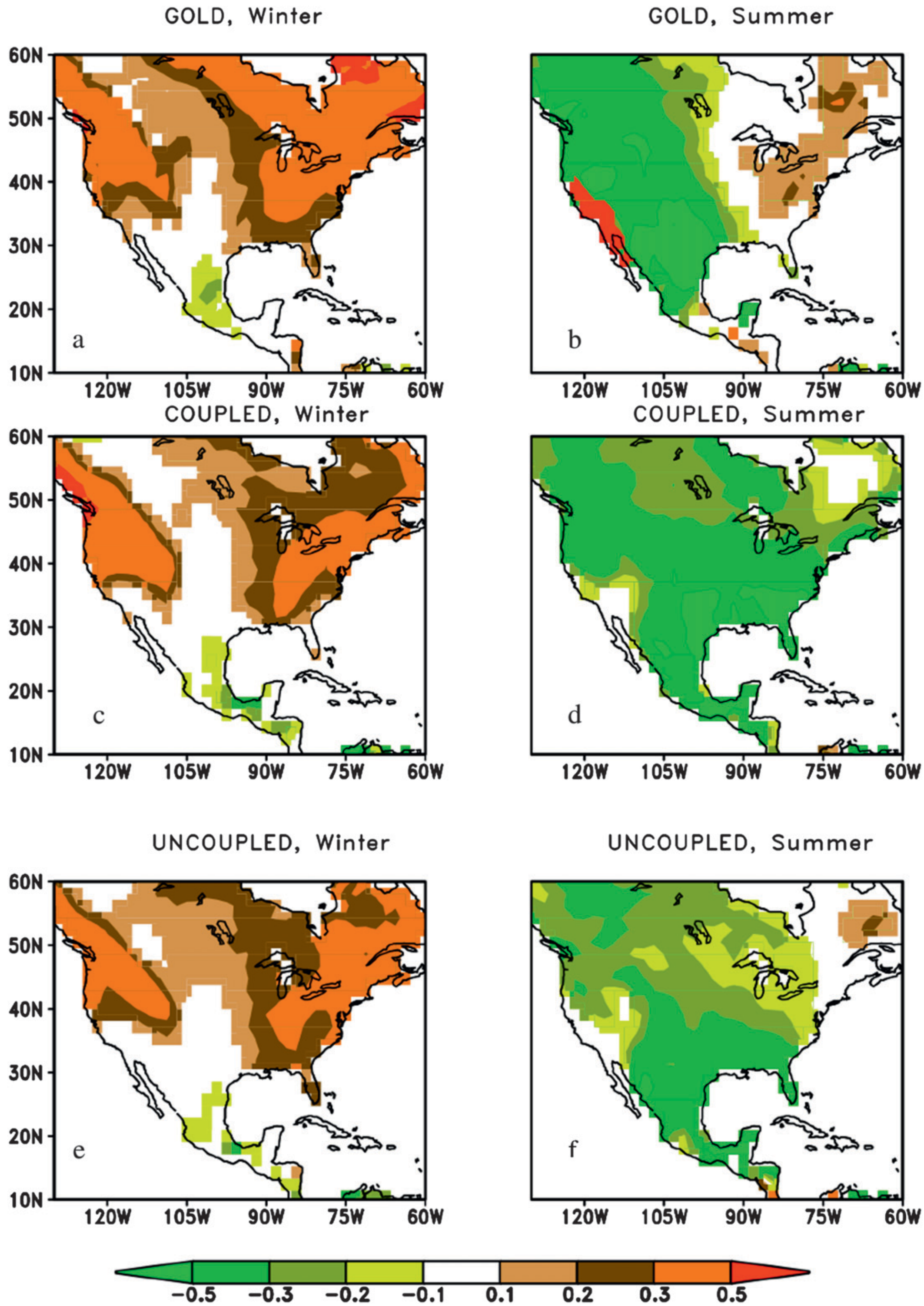

FIG. 10. Contemporaneous correlation of precipitation with surface temperature from daily values in boreal winter and boreal summer from (a),(b) GOLD, and (c),(d) COUPLED and (e),(f) UNCOUPLED simulations. Only significant values at 90% confidence interval according to the *t* test are shaded.

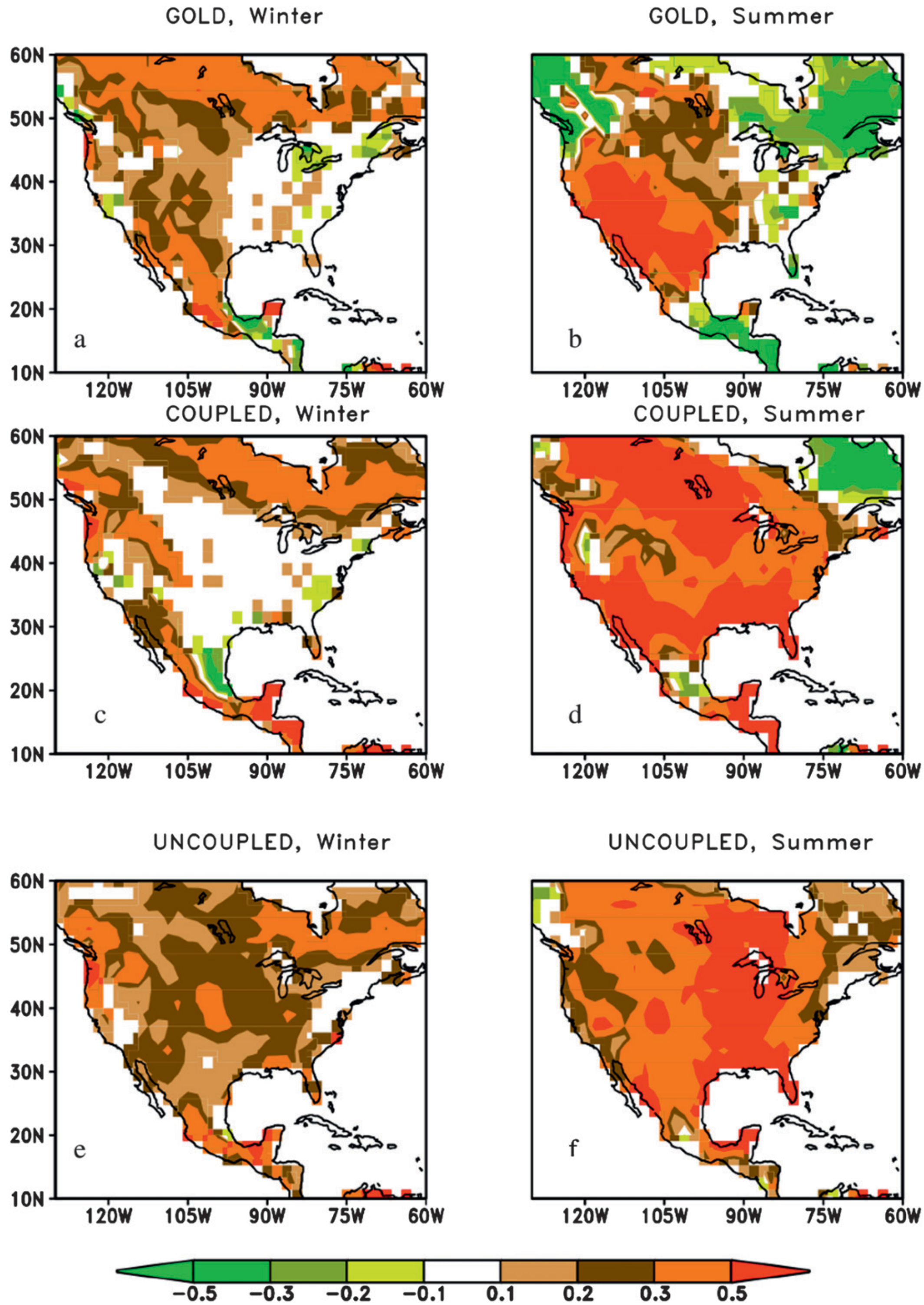

FIG. 11. Same as Fig. 10 but for correlation of precipitation with evaporation.

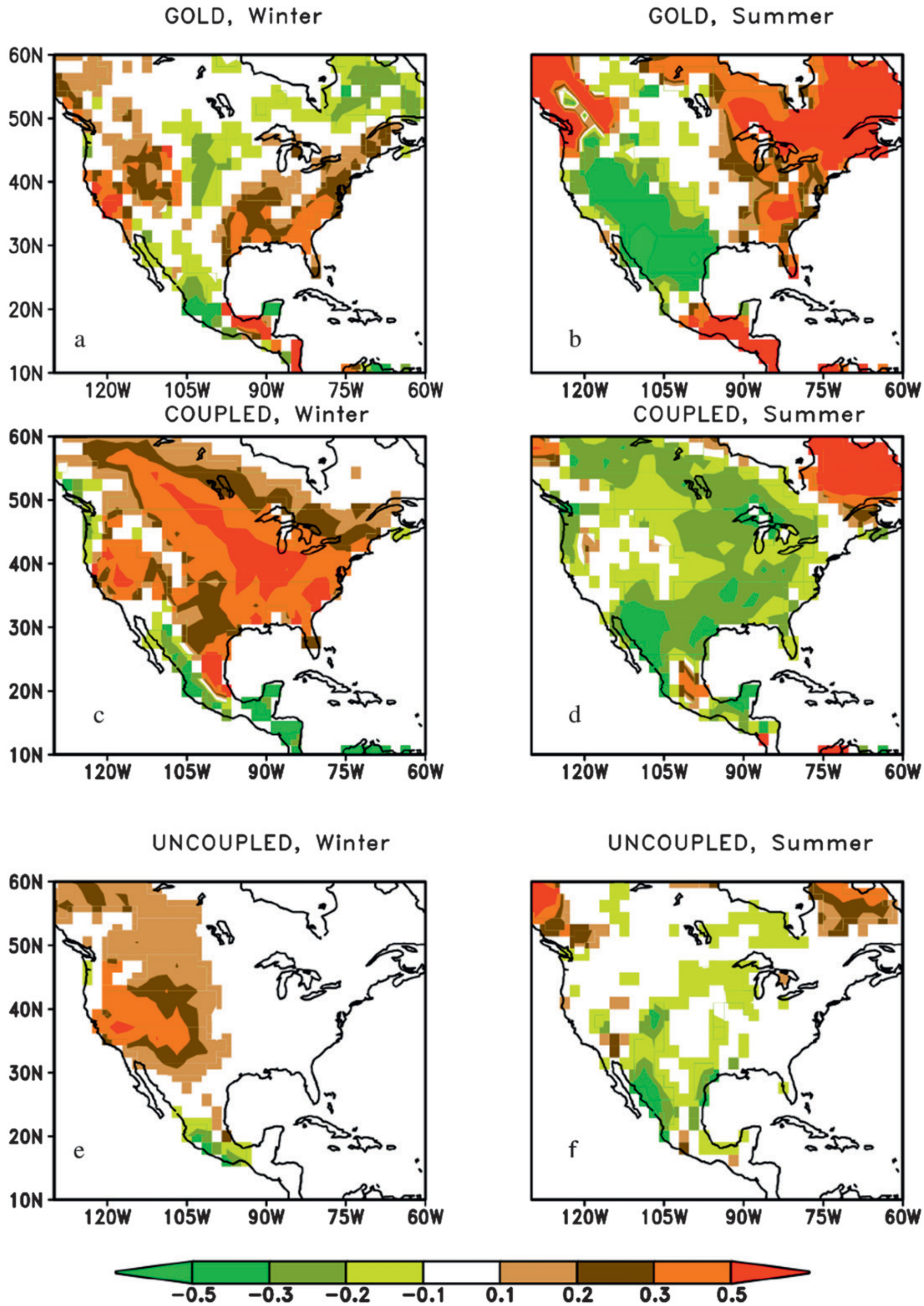

FIG. 12. Same as Fig. 10 but for correlation of downwelling shortwave flux at surface with evaporation.

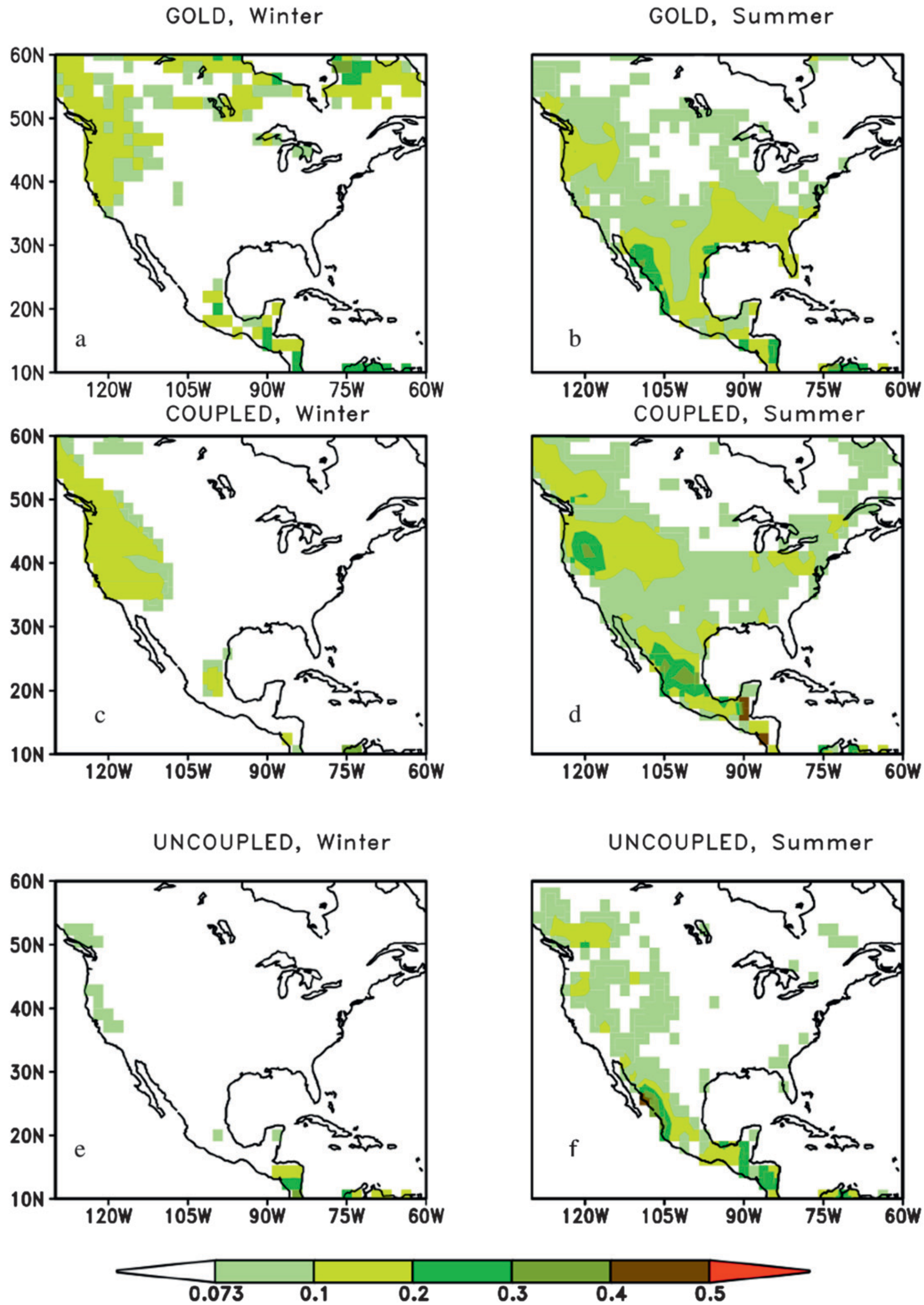

FIG. 13. The correlation of twice-removed triad precipitation amounts for winter and summer from (a),(b) GOLD, and (c),(d) COUPLED and (e),(f) UNCOUPLED simulations, respectively. Only significant values at 90% confidence interval according to the *t* test are shaded.

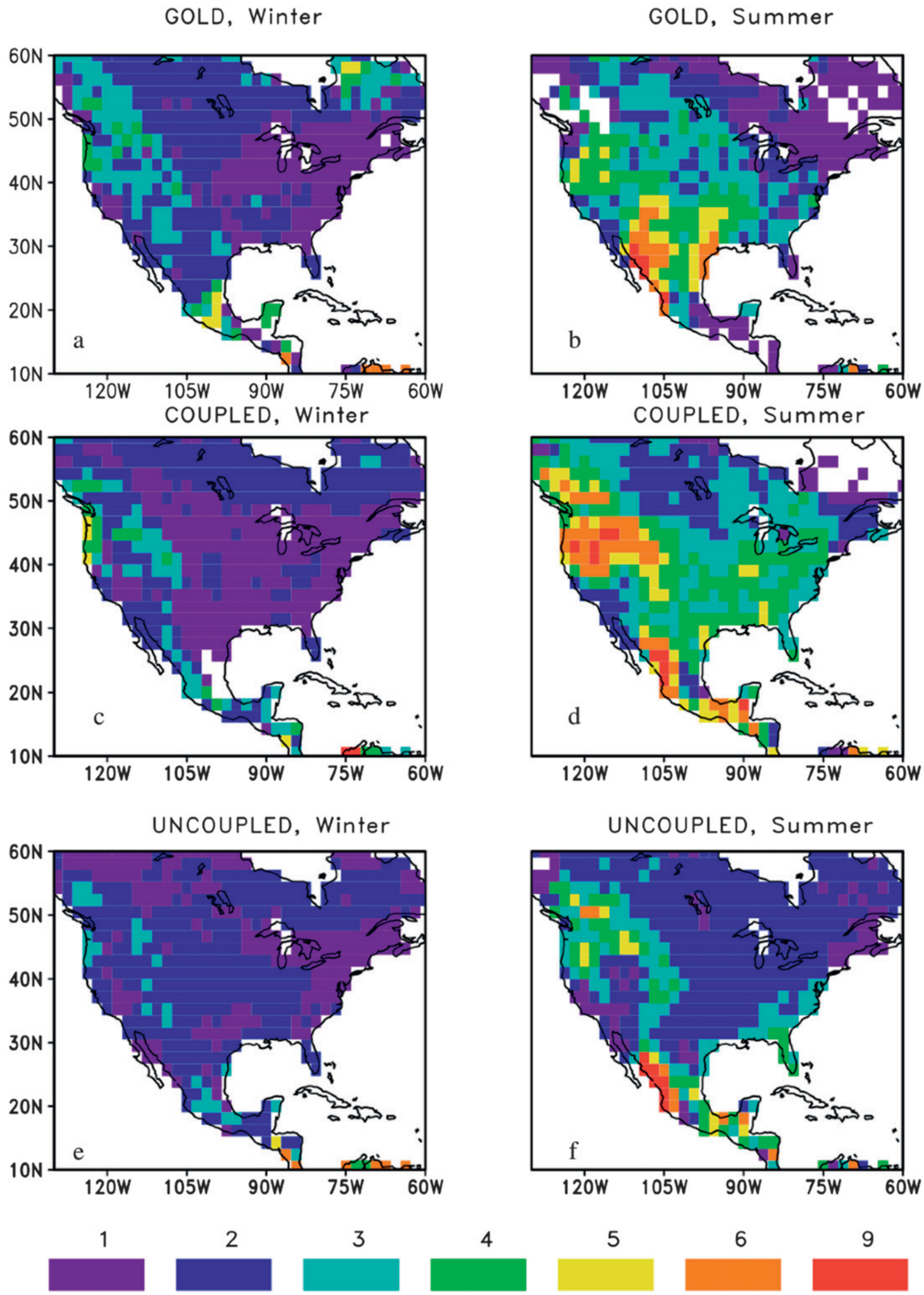

FIG. 14. The total number of days when significant correlation (according to the *t* test at 90% confidence interval) exists when evaporation leads precipitation (using daily data) in boreal winter and boreal summer from (a),(b) GOLD, and (c),(d) COUPLED and (e),(f) UNCOUPLED simulations, respectively.

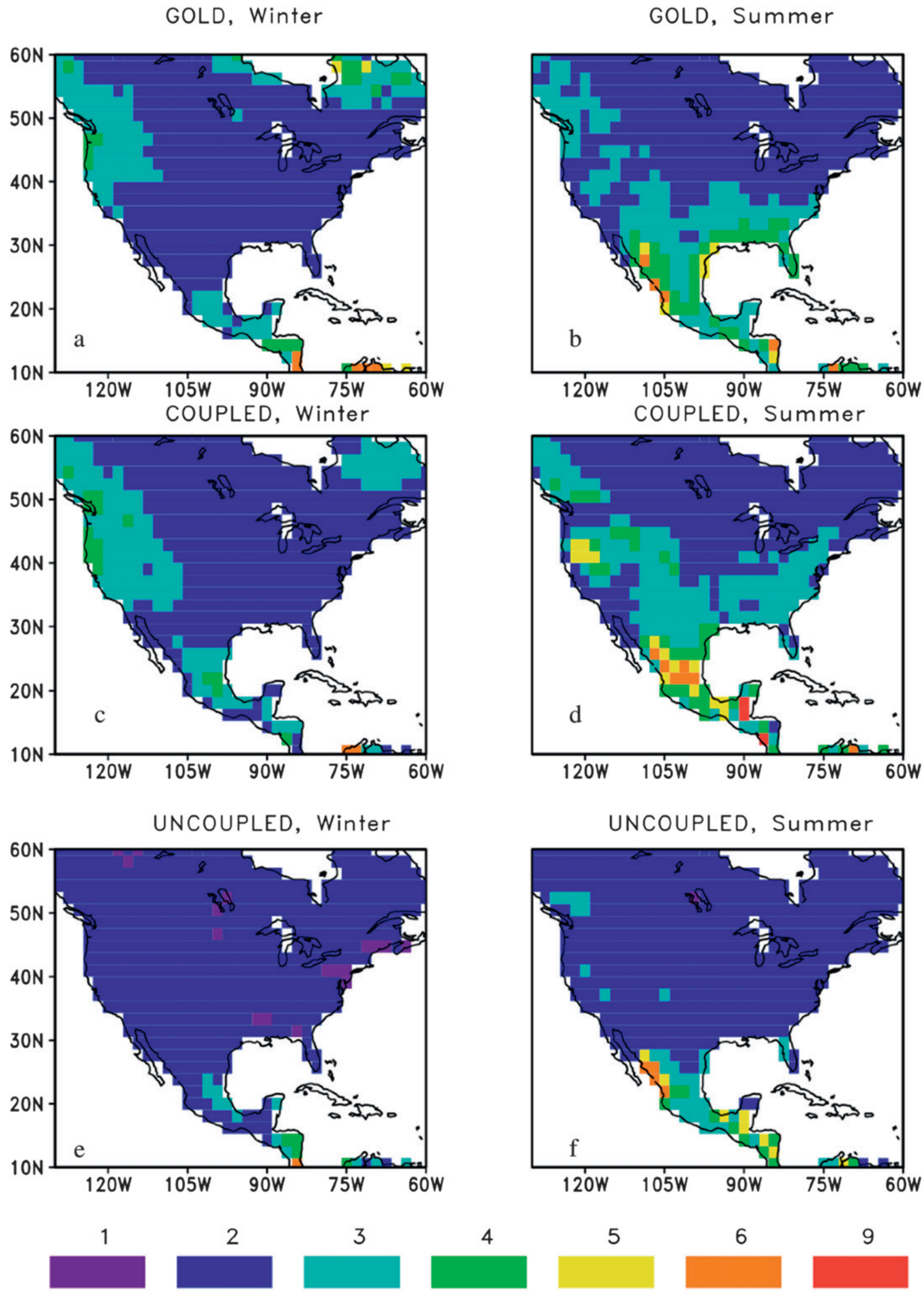

FIG. 15. Decorrelation time (days) of daily precipitation in boreal winter and boreal summer from (a),(b) GOLD, and (c),(d) COUPLED and (e),(f) UNCOUPLED simulations.

Koster et al. (2003), the correlation of twice-removed triad precipitation from GOLD, and the COUPLED and UNCOUPLED simulations. That is, it shows the average of the correlations between precipitation of one triad (say, days 1–3) and the precipitation two triads later (say, days 6–9) in a given season. Presumably, if land–atmosphere feedback contributes to prolonging rainy or dry periods, then this should be reflected in these temporal correlations. In Fig. 13a, the significant correlations are observed only in the northwestern United States. The COUPLED simulation (Fig. 13c) captures this correlation fairly well, while the UNCOUPLED simulation (Fig. 13e) completely misses it. However, in the boreal summer season, the COUPLED simulation (Fig. 13d) and GOLD data (Fig. 13b) indicate significant correlations over most parts of southern United States, suggesting a strong land–atmosphere feedback mechanism (Koster et al. 2003). The UNCOUPLED simulation shows a far less resemblance to GOLD, presumably as a result of the prevalent dry bias (Fig. 1f).

In Fig. 14, the number of contiguous days when significant correlation exists between evaporation and precipitation (with the former leading the latter) is shown for both seasons. Clearly, in Figs. 14a–d, longer lead times are seen over the North American monsoon region, northwestern United States, parts of Texas, and the southeastern United States in the boreal summer season relative to the winter season in both GOLD and the COUPLED simulation. However, unlike the COUPLED run, the UNCOUPLED simulation has a shorter lead-time between evaporation and precipitation in the summer, reflecting a model bias probably perpetuated by the deficient rainfall (Fig. 1f). In Fig. 15, the decorrelation time of daily precipitation is shown for both seasons. This decorrelation time is defined as the average time in days when the autocorrelation falls below the significance level for 90 degrees of freedom according to the *t* test. In the boreal winter season except over parts of the northwestern United States and over Central America, the decorrelation time is less than three days in the GOLD analysis (Fig. 15a). The UNCOUPLED simulation shows a larger bias in Fig. 15e (compared to the COUPLED simulation in Fig. 15c) with a much shorter decorrelation time, especially over the northwestern United States. In the boreal summer season, the decorrelation time increases over Central America and the southeastern United States in the GOLD (Fig. 15b) and in the COUPLED run (Fig. 15d), consistent with the corresponding previous figure of the lagged correlation between evaporation and precipitation (Fig. 14). The UNCOUPLED run continues to show a much shorter decorrelation time than either the GOLD or the COUPLED simulation. The two figures (Figs. 14 and 15) suggest that the increased lead-time of the influence of evaporation on precipitation in the boreal summer season is coincident with the areas of increased decorrelation time of precipitation. In other words, it implies that the land–atmosphere feedback is prolonging the duration of the wet (or dry) events in the COUPLED simulation and in the GOLD analysis.

5. Conclusions

In this study, we have compared multidecadal model runs of the COLA AGCM: one coupled to an OGCM (MOM3) and the other forced by observed SST for their simulation of the hydroclimate over the continental United States. We find that the differences in the hydroclimate over the United States in the two model runs are relatively larger in the boreal summer than in the boreal winter season. It is shown that the stronger land–atmosphere feedback in the boreal summer season augments the differences probably initiated by remote forcing. In the boreal winter (summer) season, evaporation is largely energy (moisture) limited. As a result, the U.S. hydroclimate in the boreal summer season for the most part is hydrologically more active, with equally active convective precipitation that serves as a conduit between the surface fluxes and precipitation. It should also be noted that as a result of the Clausius–Clapeyron relation, the absolute humidity in the atmospheric column is larger in the summer than in the winter. This raises the moist static energy, which gives rise to relatively stronger convective activity and potentially larger influence of boundary forcing differences on the water cycle.

The coupled ocean–land–atmosphere framework provides a new challenge to attribute climate anomalies to specific physical processes. Isolating the effect of land feedback, which was done previously with forced AGCM integrations by shutting it off artificially, is a nontrivial task in this coupled framework where the SST can also be modified. In this study, we have resorted to diagnostics that point in a somewhat subjective manner to the strong presence of land–atmosphere feedback at nearly continental scale as part of the reason for the divergence of the solutions over the United States between the COUPLED and UNCOUPLED runs.

Acknowledgments. We have benefited from useful suggestions from Dr. V. Krishnamurthy of COLA, Dr. W. J. Gutowski Jr., and two anonymous reviewers on an earlier version of the manuscript. The use of computing resources at the NASA Ames facility under Columbia project SMD05-0115 is acknowledged. This research was supported by NSF Grant 0334910, NOAA Grants NA040OAR4310034 and NA07OAR4310268, and NASA Grant NNG04GG46G.

REFERENCES

Bacmeister, J., and Coauthors, 2000: An atlas of seasonal means simulated by the NSIPP-1 atmospheric GCM. 17. NASA Tech. Memo. 104606, Goddard Space Flight Center, Greenbelt, MD, 194 pp.

Berg, A. A., J. S. Famiglietti, J. P. Walker, and P. R. Houser, 2003: Impact of bias correction to reanalysis products on simulations of North American soil moisture and hydrologic fluxes. *J. Geophys. Res.,* **108,** 4490, doi:10.1029/2002JD003334.

Collins, W. D., and Coauthors, 2006: The Community Climate System Model Version 3 (CCSM3). *J. Climate,* **19,** 2122–2143.

Dirmeyer, P. A., 2005: The land surface contribution to boreal summer season predictability. *J. Hydrometeor.,* **6,** 618–632.

——, and F. J. Zeng, 1999: Precipitation infiltration in the Simplified SiB land surface scheme. *J. Meteor. Soc. Japan,* **77,** 291–303.

——, and L. Tan, 2001: A multi-decadal global land-surface data set of state variables and fluxes. COLA Tech. Rep. 102. [Available online at ftp://grads.iges.org/pub/lba/102ctr_dirmeyer_tan.pdf.]

——, X. Gao, M. Zhao, Z. Guo, T. Oki, and N. Hanasaki, 2006: GSWP-2: Multimodel analysis and implications for our perception of the land surface. *Bull. Amer. Meteor. Soc.,* **87,** 1381–1397.

Dominguez, F., and P. Kumar, 2005: Dominant modes of moisture flux anomalies over North America. *J. Hydrometeor.,* **6,** 194–209.

Gent, P. R., and J. C. McWilliams, 1990: Isopycnal mixing in ocean circulation models. *J. Phys. Oceanogr.,* **20,** 150–155.

Guo, Z., and Coauthors, 2006: GLACE: The Global Land–Atmosphere Coupling Experiment. Part II: Analysis. *J. Hydrometeor.,* **7,** 611–625.

Higgins, R. W., Y. Chen, and A. V. Douglas, 1999: Interannual variability of the North American warm season precipitation regime. *J. Climate,* **12,** 653–680.

——, W. Shi, E. Yarosh, and J. Shaake, 2004: New orographic adjustments improve precipitation analyses for GAPP. *GEWEX News,* 14, International GEWEX Project Office, Silver Spring, MD, 8–9.

Hong, S. Y., and H. L. Pan, 1996: Nonlocal boundary layer vertical diffusion in a medium-range forecast model. *Mon. Wea. Rev.,* **124,** 2322–2339.

Huang, J., and H. M. Van den Dool, 1993: Monthly precipitation–temperature relations and temperature prediction over the United States. *J. Climate,* **6,** 1111–1132.

Kalnay, E., and Coauthors, 1996: The NCEP/NCAR 40-Year Reanalysis Project. *Bull. Amer. Soc.,* **77,** 437–471.

Kiehl, J. T., J. J. Hack, G. Bonan, B. A. Boville, D. L. Williamson, and P. J. Rasch, 1998: The National Center for Atmospheric Research Community Climate Model: CCM3. *J. Climate,* **11,** 1131–1149.

Koster, R. D., M. J. Suarez, R. W. Higgins, and H. M. Van den Dool, 2003: Observational evidence that soil moisture variations affect precipitation. *Geophys. Res. Lett.,* **30,** 1241, doi:10.1029/2002GL016571.

——, and Coauthors, 2004: Regions of strong coupling between soil moisture and precipitation. *Science,* **305,** 1138–1140.

——, and Coauthors, 2006: GLACE: The Global Land–Atmosphere Coupling Experiment. Part I: Overview. *J. Hydrometeor.,* **7,** 590–610.

Large, W. G., J. C. McWilliams, and S. C. Doney, 1994: Oceanic vertical mixing: A review and a model with a nonlocal boundary layer parameterization project. *Climate Dyn.,* **18,** 255–272.

Meehl, G., and Coauthors, 2007: The WCRP CMIP3 multimodel dataset: A new era in climate change research. *Bull. Amer. Soc.,* **88,** 1383–1394.

Misra, V., 2007: A sensitivity study of the coupled simulation of the Northeast Brazil rainfall variability. *J. Geophys. Res.,* **112,** 10.1029/2006JD008093.

——, 2008: Coupled interactions of the monsoons. *Geophys. Res. Lett.,* **35,** L12705, doi:10.1029/2008GL033562.

——, and L. Marx, 2007: Manifestation of remote response over equatorial Pacific in a climate model. *J. Geophys. Res.,* **112,** D20105, doi:10.1029/2007JD008597.

——, and Coauthors, 2007: Validating and understanding ENSO simulation in two coupled climate models. *Tellus,* **59A,** 292–308.

Moorthi, S., and M. Suarez, 1992: Relaxed Arakawa–Schubert: A parameterization of moist convection for general circulation models. *Mon. Wea. Rev.,* **120,** 1441–1467.

Nigam, S., 2003: Teleconnections. *Encyclopedia of Atmospheric Sciences*, J. R. Holton, J. A. Pyle, and J. A. Curry, Eds., Elsevier Science, Vol. 6, Academic Press, Elsevier Science, 2243–2269.

——, M. Barlow, and E. H. Berbery, 1999: Pacific decadal SST variability: Impact on U.S. drought and streamflow. *Eos, Trans. Amer. Geophys. Union,* **80,** 621–625.

Pacanowski, R. C., and S. M. Griffies, 1998: MOM3.0 manual. NOAA/Geophysical Fluid Dynamics Laboratory, 638 pp.

Redi, M. H., 1982: Oceanic isopycnal mixing by coordinate rotation. *J. Phys. Oceanogr.,* **12,** 1154–1158.

Reynolds, R. W., N. A. Rayner, T. M. Smith, D. C. Stokes, and W. Wang, 2002: An improved in situ and satellite SST analysis for climate. *J. Climate,* **15,** 1609–1625.

Rudolf, B., H. Hauschild, W. Reuth, and U. Schneider, 1994: Terrestrial precipitation analysis: Operational method and required density of point measurements. *Global Precipitation and Climate Change,* M. Desbois, F. Desalmond, Ed., NATO ASI Series I, Vol. 26, Springer-Verlag, 173–186.

Ruiz-Barradas, A., and S. Nigam, 2005: Warm season rainfall variability over the U.S. Great Plains in observations, NCEP and ERA-40 reanalysises, and NCAR and NASA atmospheric model simulations. *J. Climate,* **18,** 1808–1830.

——, and ——, 2006: Great Plains hydroclimate variability: The view from North American regional reanalysis. *J. Climate,* **19,** 3004–3010.

Saha, S., and Coauthors, 2006: The Climate Forecast System at NCEP. *J. Climate,* **19,** 3483–3517.

Shukla, J., and Y. Mintz, 1982: Influence of land–surface evapotranspiration on the earth's climate. *Science,* **215,** 1498–1501.

Slingo, J. M., 1987: The development and verification of a cloud prediction model for the ECMWF model. *Quart. J. Roy. Meteor. Soc.,* **113,** 899–927.

Smagorinsky, J., 1963: General circulation experiments with the primitive equations: I. The basic experiment. *Mon. Wea. Rev.,* **91,** 99–104.

Tiedtke, M., 1984: The effect of penetrative cumulus convection on the large-scale flow in a general circulation model. *Beitr. Phys. Atmos.,* **57,** 216–239.

Trenberth, K. E., and C. J. Guillemot, 1996: Physical processes involved in the 1988 drought and 1993 floods in North America. *J. Climate,* **9,** 1288–1298.

——, L. Smith, T. Qian, A. Dai, and J. Fasullo, 2007: Estimates of the global water budget and its annual cycle using observational and model data. *J. Hydrometeor.,* **8,** 758–769.

Voldoire, A., and J.-F. Royer, 2005: Climate sensitivity to tropical land surface changes with coupled versus prescribed SSTs. *Climate Dyn.,* **24,** 843–862.

Xue, Y. K., P. J. Sellers, J. L. Kinter III, and J. Shukla, 1991: A simplified biosphere model for global climate studies. *J. Climate,* **4,** 345–364.

——, F. J. Zeng, and C. A. Schlosser, 1996: SSiB and its sensitivity to soil properties—A case study using HAPEX-Mobilhy data. *Global Planet. Change,* **13,** 183–194.